Construction and Building Materials 23 (2009) 2346–2356

Contents lists available at ScienceDirect

Construction and Building Materials

journal homepage: www.elsevier.com/locate/conbuildmat

Performance evaluation of rebar in chloride contaminated concrete by corrosion rate

Bulu Pradhan [a,*], B. Bhattacharjee [b]

[a] Department of Civil Engineering, Indian Institute of Technology Guwahati, Guwahati 781 039, India
[b] Department of Civil Engineering, Indian Institute of Technology Delhi, New Delhi 110 016, India

ARTICLE INFO

Article history:
Received 17 August 2008
Received in revised form 29 October 2008
Accepted 4 November 2008
Available online 16 December 2008

Keywords:
Concrete
Cement
Steel
Corrosion rate
LPR
AC impedance spectroscopy
Gravimetric measurement

ABSTRACT

The presence of chloride ions in reinforced concrete (RC) plays a major role in reinforcement corrosion and hence for the durability and service life of RC structures. With growing concern towards the deterioration of reinforced concrete structures, the use of electrochemical techniques for their performance evaluation has become an important topic of durability study. This paper illustrates the findings of an experimental investigation carried out on large number of specimens for evaluating the performance of different types of rebar in chloride contaminated concrete made with different types of cement through different corrosion rate techniques. The specimens were prepared with three types of cement and three types of steel. From the results of corrosion rate, it was observed that the values of corrosion rate obtained by linear polarization resistance (LPR) technique with guard ring arrangement were in close agreement with those obtained by gravimetric method. On the other hand the corrosion rate values obtained by AC impedance spectroscopy were slightly lower than those obtained by LPR measurement. Further, correlations between different corrosion rate techniques were also obtained. From the results of analysis of variance (ANOVA), it was observed that chloride content has the strongest effect on corrosion rate as compared to other factors.

1. Introduction

Reinforced concrete structures provide excellent service under certain environmental conditions. In well made and good quality concrete the risk of corrosion is minimal as it normally provides good chemical and physical protection to the embedded steel reinforcement [1,2]. The chemical protection is through the formation of a passive layer (thin protective oxide film) over the steel surface due to high alkalinity of concrete pore solution while the physical protection is through the retarding access of oxygen, moisture, and various aggressive species to the steel/concrete interface. However the breakdown of the passive film and consequently corrosion initiation takes place most frequently in the presence of chloride ions at the rebar level. The aggressive chloride ions can be originated either from the use of contaminated mix ingredients in the mix and/or from the surrounding environment in the hardened state.

The corrosion of rebar in concrete is generally considered as an electrochemical process [3–7]. With the attention of researchers focusing towards the prediction of the residual life of reinforced concrete structures affected by the reinforcement corrosion, the use of electrochemical techniques for the determination of relevant parameters in this regard becomes a major area of durability study. Therefore nowadays the electrochemical techniques are widely used for the study of rebar corrosion in laboratories together with their application to real life structures [8]. In addition it is necessary to evaluate the short-term performance of different structures to know their early age behaviour by performing various corrosion tests at initial periods, for prognosis of possible deterioration so as to estimate the projected service life.

Corrosion rate is an important parameter for quantitatively predicting the service life of reinforced concrete structures which is limited by the corrosion deterioration. Thus the performance of different types of rebar against corrosion in chloride contaminated concrete made with different types of cement can be evaluated by measuring the corrosion rate, so that the best possible combinations of cement and steel can be recommended for use in aggressive chloride environments. The various non-destructive techniques used for the determination of corrosion rate are linear polarization resistance (LPR) method, AC impedance spectroscopy and Tafel plot technique. The gravimetric (mass loss) measurement is a destructive technique for obtaining the corrosion rate. LPR technique provides a simple method for the determination of corrosion rate both in the laboratory and field studies. In LPR measurements, the steel reinforcement is polarized by the application of a small perturbation from the equilibrium potential through an auxiliary electrode. The polarized surface area of the reinforcing steel is assumed to be that area which lies directly below the auxiliary electrode. However there is considerable evidence that current flowing from the auxiliary electrode is not confined and

* Corresponding author. Tel.: +91 361 258 2425; fax: +91 361 258 2440.
E-mail addresses: bulu@iitg.ernet.in, bulu_pradhan@rediffmail.com (B. Pradhan).

0950-0618/$ - see front matter © 2008 Elsevier Ltd. All rights reserved.
doi:10.1016/j.conbuildmat.2008.11.003

can spread laterally over an unknown large area of the reinforcing steel, which may lead to the inaccurate estimation of the corrosion rate [9,10]. Therefore in order to avoid the problem of the confinement of the current to predetermined area of the reinforcing steel, the use of a second auxiliary guard ring electrode surrounding the inner auxiliary electrode has been developed. The principle is to maintain the confinement current by the outer guard ring electrode during LPR measurement. This confinement current prevents the perturbation current from central auxiliary electrode spreading beyond a known area.

Due to the sophistication of the measurement, AC impedance spectroscopy technique is more frequently used in laboratory studies rather than in field surveys. Further, often it is difficult to interpret and is a time-consuming technique. Nevertheless, this technique is used as a powerful tool to understand the behaviour of the steel/concrete interface and provides information about corrosion rate of the steel reinforcement [11–14]. Visual observation and gravimetric (mass loss) measurement are also used as performance evaluation techniques. Visual observation gives qualitative results about corrosion performance of different types of steel embedded in concrete made with different types of cement. On the other hand, gravimetric (mass loss) measurement is used as a destructive test, generally conducted in laboratory. However it serves as the most reliable reference method. It is simple, although a time-consuming technique for determination of corrosion rate. The corrosion rate obtained by different non-destructive electrochemical techniques must be compared with those obtained from the gravimetric measurement.

From the reported literature, it is observed that the work on the corrosion performance of different types of cement and rebar individually in chloride contaminated concrete using various corrosion rate techniques is scanty. In addition the work on the performance evaluation of various combinations of cement and rebar by different corrosion rate techniques against chloride induced corrosion is also very little. Therefore a study involving the performance evaluation of different type of cement, steel and their combinations against chloride environment using different corrosion rate techniques can furnish useful information regarding the selection of suitable cement–steel combinations and also provide the correlation between different corrosion rate techniques. Hence one of the objectives of the present work is to determine the corrosion rate by two different electrochemical non-destructive techniques namely LPR and AC impedance spectroscopy and comparing the corrosion rate with those obtained from gravimetric (mass loss) measurement carried out on large number of specimens made with different types of steel and cement. The second objective is to appraise the performance of different types of steel, cement and their combinations on the basis of the corrosion rate results obtained from the above three methods at varying w/c ratios and varied dosages of internal chloride and proposing the best cement, steel and their combinations for use in aggressive chloride environment.

2. Experimental work

2.1. Materials and specimens

To improve the reliability of variation of corrosion rate, the experimental investigation was conducted over a wide range of parameters. For this purpose three types of cement, three types of steel, three w/c ratios and four admixed chloride contents were used for the preparation of reinforced concrete specimens. Three types of cement used were ordinary Portland cement (OPC), Portland pozzolana cement (PPC) and Portland slag cement (PSC). The chemical compositions of the three types of cement are presented in Table 1. Steel bars of diameter 12 mm were used as steel reinforcement. Three types of steel reinforcement used were cold twisted deformed (CTD) bars, Tempcore TMT bars and Thermex TMT bars. The carbon (C) content, phosphorus (P) content and sulphur (S) content of CTD, Thermex TMT and Tempcore TMT steels used in the present investigation are 0.22%, 0.044% and 0.037%; 0.19%, 0.046% and 0.029%; and 0.20%, 0.021% and 0.044%, respectively.

Table 1
Chemical composition of cement.

Compound	OPC	PPC	PSC
CaO (%)	62.1	47.72	44.36
SiO_2 (%)	21.14	28.82	30.1
Al_2O_3 (%)	5.23	9.31	10.2
Fe_2O_3 (%)	4.42	4.6	3.4
MgO (%)	1.14	1.48	4.12
SO_3 (%)	2.3	2.1	2.18
LOI (%)	1.5	2.7	1.8

The chloride was admixed into concrete as sodium chloride of analytical reagent grade. The concentrations of sodium chloride used were 0%, 1.5%, 3% and 4.5% by mass of cement and the corresponding chloride concentrations were 0%, 0.91%, 1.82% and 2.73%, respectively. Coarse aggregates of size 20 mm MSA (maximum size of aggregate) and 10 mm MSA of quartzite origin were used in the ratio of 1.78:1 to satisfy the overall grading requirement of coarse aggregate as per IS 383-1970 [15]. Land quarried sand conforming to zone II classification of British standard was used as fine aggregate. Tap water from laboratory of deep ground water source was used for the preparation of specimens. All the concrete mixes were designed for similar workability with slump of 30–60 mm. A number of trial tests were conducted to get the desired slump with different water contents and finally the water content was kept constant to 210 kg/m^3 for the desired slump in all the mixes to have similar workability. Three water–cement ratios (w/c) used were 0.45, 0.50, and 0.55. The cement contents for different concrete mixes were calculated by dividing the water content by the corresponding w/c ratios. The wet density of concrete was then obtained as per guidelines specified by British method of mix design (DOE) [16]. After that the aggregate contents were calculated. The w/c ratio, cement content, water content, fine aggregate content and coarse aggregate content of the concrete mixes made with three types of cement i.e. OPC, PPC and PSC are presented in Table 2.

The slab specimens of size 300 mm × 300 mm × 52mm were prepared with a centrally embedded steel specimen. The line diagram of the slab specimen is shown in Fig. 1. The procedure for preparation of steel specimen is similar to the guidelines specified in ASTM G109-99a [17] and also provided in an earlier paper [18]. For

Table 2
Concrete mix proportions for OPC, PPC and PSC.

Water–cement ratio (w/c)	Water content (kg/m^3)	Cement content (kg/m^3)	Fine aggregate content (kg/m^3)	Coarse aggregate content (kg/m^3)
0.45	210	466.67	596.16	1107.17
0.50	210	420.00	612.50	1137.50
0.55	210	381.82	625.86	1162.32

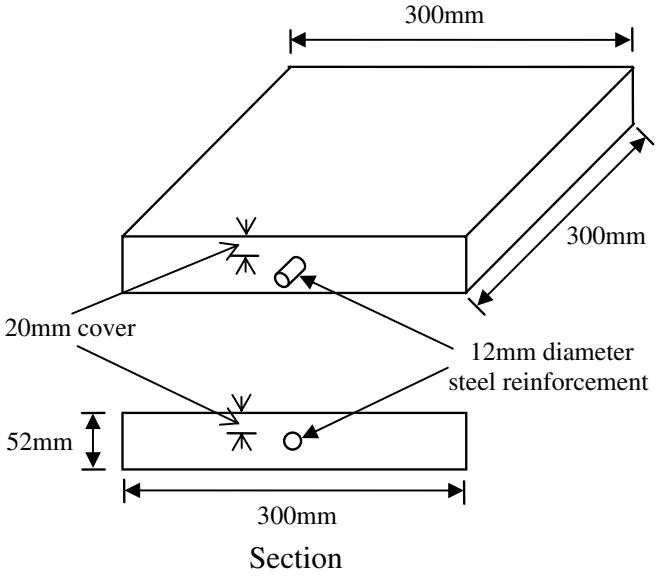

Fig. 1. Slab specimen.

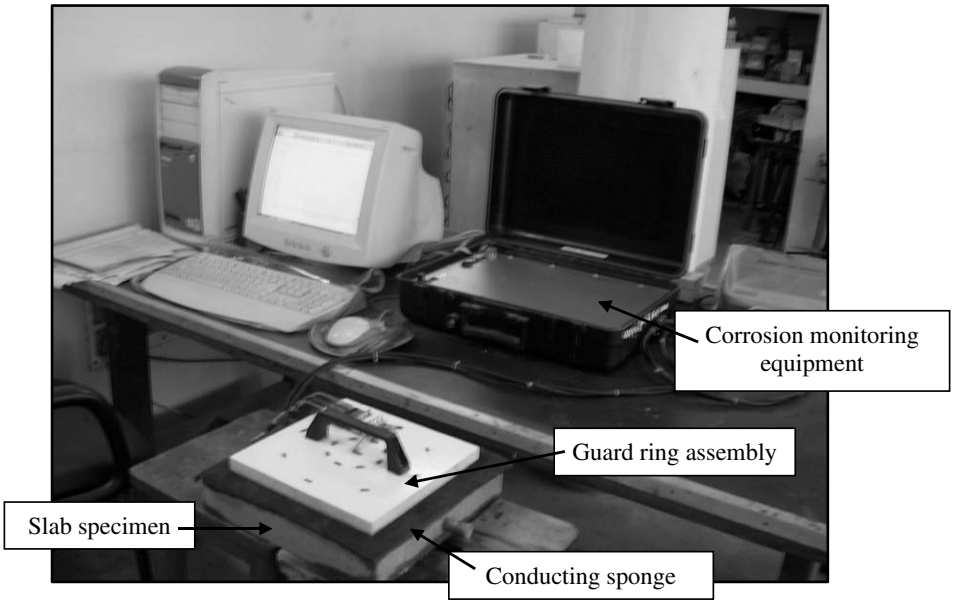

Fig. 2. Experimental arrangement for LPR measurement with guard ring assembly.

preparation of steel specimens, the steel bars were cut to the required length of 360 mm and were drilled and threaded at one end to accommodate the coarse threaded stainless steel screws. The steel bars were then wire brushed to remove any surface scale and then cleaned by soaking in analytical reagent grade hexane and allowed to air dry. After that, one stainless steel screw was attached to each cleaned steel bar. Insulating tap was then applied on each end of the bar, so that the central portion of length 250 mm of the steel bar remains bare. Neoprene tube of internal diameter 12 mm and thickness 3 mm was applied over the insulating tap for a length of 55 mm at each end of the steel bar. Epoxy was then filled in the protruded length of the neoprene tube beyond the steel bar and also applied at the inner end of the neoprene tube over the rebar.

With three types of cement, three w/c ratios, four admixed chloride contents, total 36 concrete mixes were prepared. From these 36 concrete mixes, with three types of steel and three replicates, total 324 numbers of slab specimens were prepared. After completion of moist curing (for 27 days after 24 h of preparation), the slab specimens were kept in the ambient laboratory conditions (temperature: 25–35 °C and relative humidity: 60–80%) till testing. Linear polarization resistance test was conducted on all 324 slab specimens at the ages of 60 days and 1 year. In addition LPR test was also conducted on some slab specimens at ages of 90 days and 120 days. Corrosion rate by gravimetric (mass loss) measurement was carried out on all 324 slab specimens at the age of 1 year after completion of LPR test. AC impedance spectroscopy test was performed at the age of 60 days. For the purpose of AC impedance test, additional 108 slab specimens were prepared with three types of cement, three types of steel, four admixed chloride contents, one w/c ratio, i.e. 0.5 and three replicates.

2.2. Corrosion rate

Corrosion rate of steel reinforcement was determined by three different tests namely linear polarization resistance test, AC impedance spectroscopy and gravimetric (mass loss) measurement. The electrochemical tests were performed on the slab specimens using a corrosion monitoring equipment (Make ACM, model: serial no. 993 field machine).

2.2.1. Corrosion rate by LPR technique

As concrete is a high resistive medium, the IR drop in the cover concrete is significant and may vary from specimen to specimen. Hence the IR drop value of the cover concrete needs to be determined and compensated for determining the corrosion current density. The LPR measurement with IR compensation technique used by the corrosion instrument automatically calculates the equivalent IR value of the cover concrete and compensates while determining the corrosion current density. Before performing the test, conducting sponge was wetted with soap solution and placed on the surface of the slab specimen to have proper electrical contact with the guard ring. Guard ring assembly was then placed above the wetted sponge. The polarized surface area of the steel reinforcement is taken to be that lying under a circle intersecting the midpoint between the two sensor electrodes [10] and only the top half surface area of the steel reinforcement has been assumed to be polarized [11]. For linear polarization resistance measurement, the working electrode, i.e. the steel reinforcement in the slab specimen was polarized to ±20 mV from the equilibrium potential at a scan rate of 0.1 mV per second. The experimental arrangement for LPR measurement with guard ring assembly is shown in Fig. 2.

For calculation of the corrosion current density I_{corr}, Stern-Geary equation was used

$$I_{corr} = B/R_p \tag{1}$$

where B is the Stern-Geary constant and is given by $B = (\beta_a \times \beta_c)/2.3(\beta_a + \beta_c)$. β_a and β_c are anodic and cathodic Tafel constants, respectively. The value of B was taken as 26 mV considering steel in active condition [19–23]. R_p is the polarization resistance.

2.2.2. Corrosion rate by AC impedance spectroscopy

For determination of corrosion current density using AC impedance spectroscopy, a sinusoidal voltage of amplitude 5 mV was applied in the frequency range of 0.01–30000 Hz to all the specimens. The test set-up and electrodes used for this technique are same as that used for LPR test. For calculation of the corrosion current density, the assumed model for the steel/concrete interface is shown in Fig. 3. The steel–concrete interface is represented by a simple equivalent electric circuit. The equivalent circuit consists of concrete resistance R_c in series with the interface impedance [11]. The interface impedance consists of polarization resistance R_p in parallel with a double layer capacitance C. The frequency dependent impedance $Z(\omega)$ of the electrical equivalent circuit shown in Fig. 3 is given by the following expression:

$$Z(\omega) = R_c + \frac{R_p}{(1+\omega^2 R_p^2 C^2)} - \frac{j\omega C R_p^2}{(1+\omega^2 R_p^2 C^2)} \tag{2}$$

where ω = angular frequency of the applied signal, C = double layer capacitance.

From the above equation, the value of $Z(\omega)$ at very low frequencies becomes

$$Z_{\varpi \to 0}(\omega) = R_c + R_p \tag{3}$$

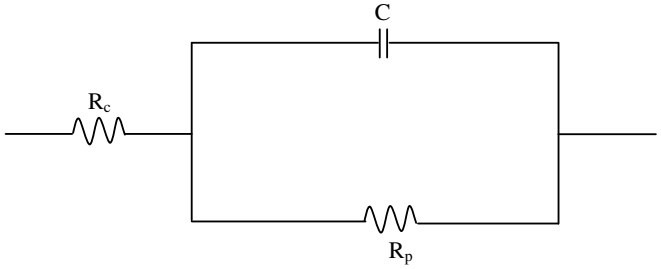

Fig. 3. Equivalent electric circuit for steel/concrete interface.

and at very high frequencies

$$Z_{\varpi \to \infty}(\omega) = R_c \quad (4)$$

Therefore R_c measured at high frequency can be subtracted from $R_p + R_c$ measured at low frequency to give a compensated value of R_p free of ohmic interferences in high resistivity medium like concrete.

The impedance behaviour of an electrode may be expressed in Nyquist plots of $Z''(\omega)$ (imaginary component) as a function of $Z'(\omega)$ (real component) or in Bode plots of impedance and θ (phase angle) versus $\log(\omega)$. The Nyquist plot shows a semicircle with frequency increasing in a counterclockwise direction. At very high frequency, the imaginary component $Z''(\omega)$disappears, leaving only the concrete resistance, R_c. At very low frequency, $Z''(\omega)$ again disappears leaving a sum of R_c and R_p. Thus the radius of the semi circle is $R_p/2$. Typical Nyquist plots obtained from the test are shown in Figs. 4a and 4b. An experimentally obtained Bode plot is shown in Fig. 5. The value of the Stern-Geary constant "*B*" was again taken as 26 mV for calculating the corrosion current density considering steel in active condition [19–23].

2.2.3. Corrosion rate by gravimetric (mass loss) measurement

For the determination of corrosion rate by gravimetric (mass loss) measurement, the slab specimens were broken at the age of 1 year after completion of LPR test. The set-up used for breaking of specimens is shown in Fig. 6. Prior to cleaning, steel specimens removed from slab specimens were visually observed for corrosion. The procedure stated in ASTM G 1-03 [24] was adopted for the cleaning of the corroded steel specimens and for determination of mass loss. The time period for calculation of the mass loss was taken as 338 days (365-27). This is because initially the slab specimens were completely moist cured in a curing tank for 27 days after 24 h of preparation and during this period there was lack of oxygen for corrosion reactions to take place. For the purpose of cleaning, the cleaning solution used was 500 ml of hydrochloric acid with 3.5 gm of hexamethylene tetramine added with reagent water to make it 1000 ml. Each specimen was cleaned several times with this solution and mass loss was noted after each cleaning. The cleaning period was selected as 2 min for each cleaning. A typical plot of mass loss versus cleaning time obtained from the experiment is shown in Fig. 7. The mass loss corresponding to the cleaning time after which no significant increase in mass loss observed was used for calculation of corrosion rate as shown in Fig. 7 through a backward extrapolation.

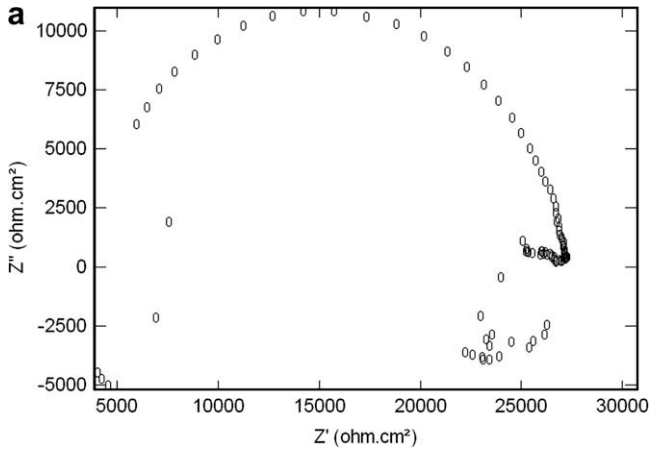

Fig. 4a. A typical experimentally obtained Nyquist plot (for PPC, CTD steel, w/c = 0.5, 0%Chloride).

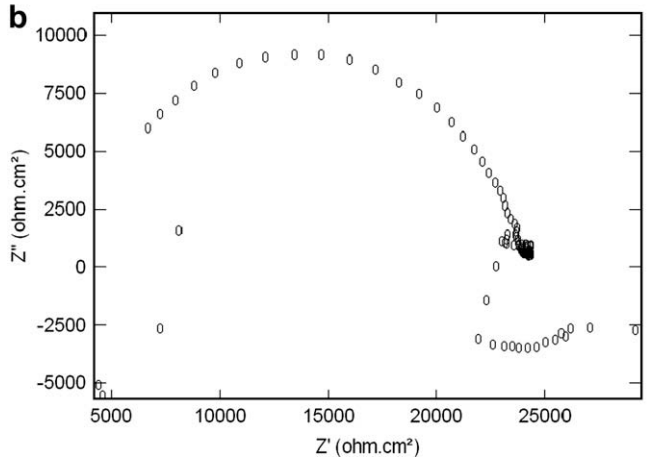

Fig. 4b. A typical experimentally obtained Nyquist plot (for OPC, Tempcore TMT steel, w/c = 0.5, 0%Chloride).

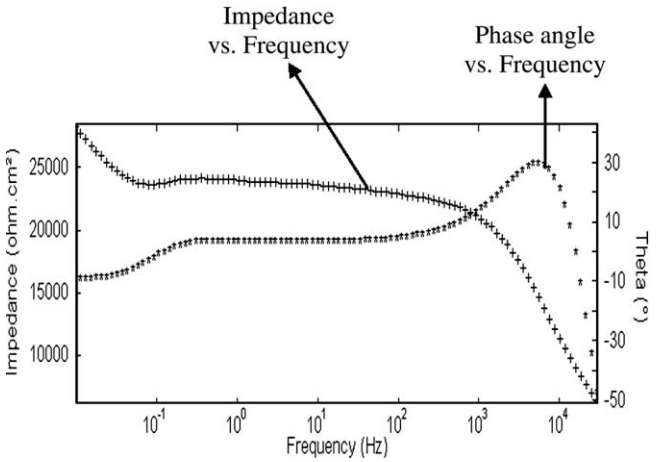

Fig. 5. A typical experimentally obtained Bode plot (for OPC, CTD steel, w/c = 0.5, 0% Chloride).

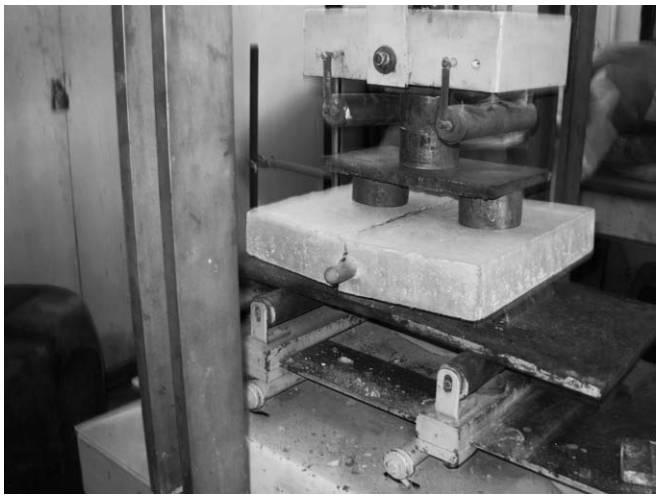

Fig. 6. Set-up for breaking of slab specimens.

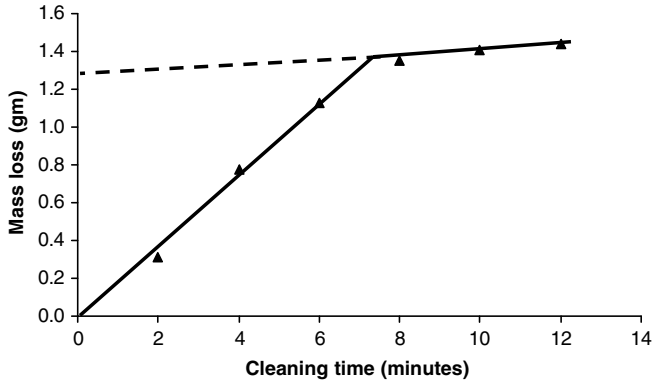

Fig. 7. A typical experimentally obtained plot of mass loss versus cleaning time.

The corrosion rate was calculated using the following equation given in ASTM G 1-03 [24]

$$\text{Corrosion rate (mm/year)} = \frac{(K \times W)}{(A \times T \times D)} \quad (5)$$

where K = a constant equal to 8.76×10^4, W = mass loss in grams, A = actual corroded area of steel bar in cm^2 after removal from slab specimen and visually examining, T = time of exposure in hours, D = density of steel, i.e. 7.85 g/cm^3.

For the purpose of comparison, using Faraday's law, the corrosion rate in mm/year obtained from gravimetric (mass loss) measurement was converted to corrosion current density ($\mu A/cm^2$) by assuming uniform corrosion occurred over the steel surface by the following equation [11–13,25]:

$$\text{Corrosion rate (mm/year)} = \frac{0.00327 \times a \times I_{corr}}{n \times D} \quad (6)$$

where I_{corr} = corrosion current density in $\mu A/cm^2$, a = atomic weight of iron, i.e. 55.84 amu, n = no. of electrons exchanged in corrosion reaction, i.e. 2 for iron, D = density of steel as above.

3. Results and discussion

3.1. Corrosion rate by LPR technique

The corrosion current density values indicate the progress of corrosion and consequently indicate the performance of different types of steel and cement in propagation phase of service life. From the results it was observed that the corrosion current density increased with increase in free chloride concentration. The procedure for determination and results of free chloride contents for different concrete mixes are provided in an earlier paper [18]. The average corrosion current density value at different free chloride contents for each cement type individually was calculated by taking the average of corrosion current density values (obtained at the age of 60 days by LPR technique) over all steels, w/c ratios and replicates. Similarly while calculating the average corrosion current density for each steel type individually, the average value was calculated over all types of cement and w/c ratios as replicates. These average corrosion current density values were plotted against the corresponding free chloride concentrations and are shown along with their corresponding relationships in Figs. 8 and 9 for three types of steel and three types of cement, respectively. From Fig. 8 it is observed that Tempcore TMT steel exhibited lower values of corrosion current density than those exhibited by Thermex TMT and CTD steels at almost all levels of free chloride concentrations. The difference in the corrosion current density values between Tempcore TMT steel and Thermex TMT steel and that between Tempcore TMT steel and CTD steel increased with increase in free chloride content as evident from Fig. 8. In other words the rate of increase in corrosion current density with free chloride content is

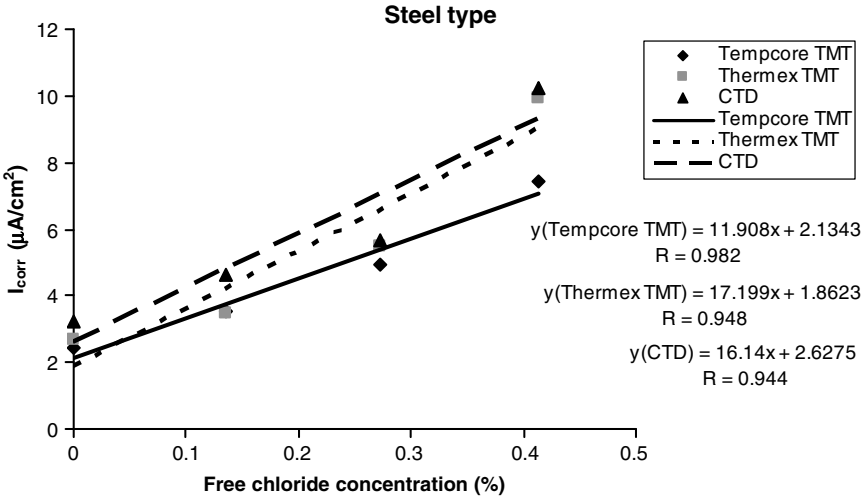

Fig. 8. Average corrosion current density versus free chloride content for three types of steel.

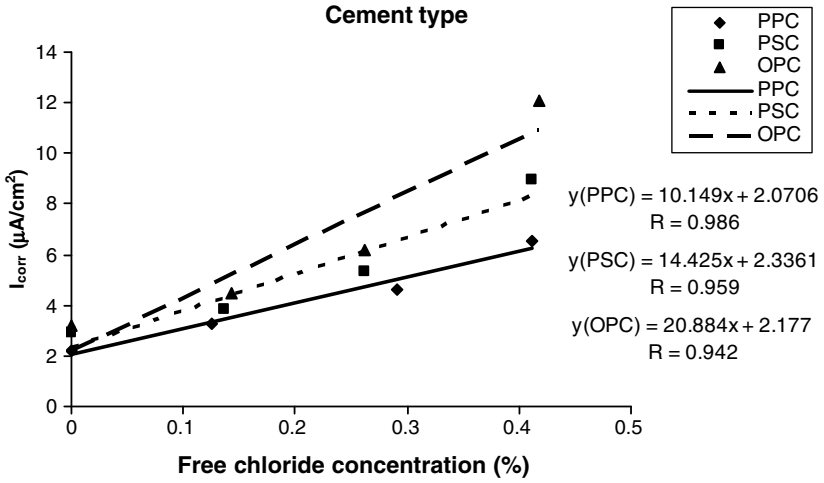

Fig. 9. Average corrosion current density versus free chloride content for three types of cement.

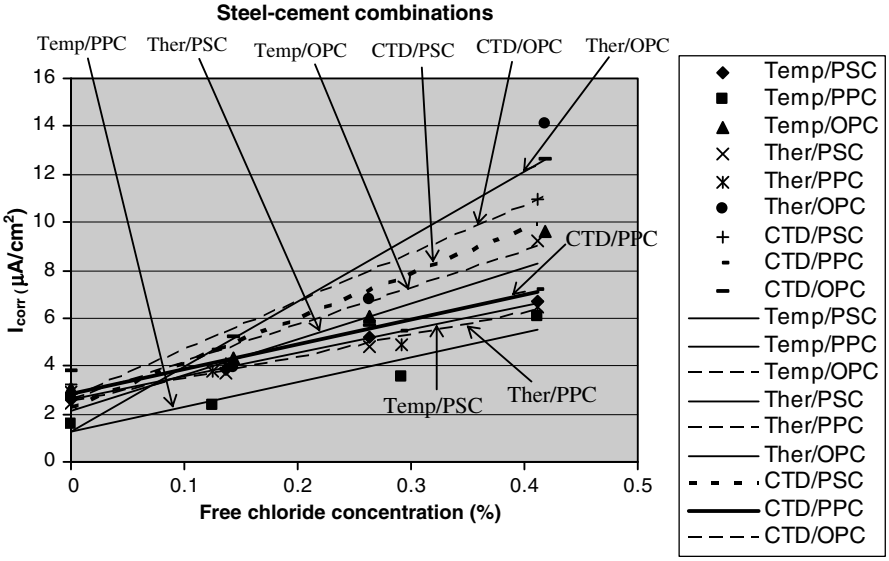

Fig. 10. Average corrosion current density versus free chloride content for steel–cement combinations.

less for Tempcore TMT steel than for other two steels as indicated by the slopes of respective relationships shown in Fig. 8. On comparing Thermex TMT steel and CTD steel, the former exhibited lower average corrosion current density values than the latter. On the other hand amongst cement type, PPC exhibited lower corrosion current density values than those exhibited by PSC and OPC at all levels of free chloride content as observed from Fig. 9. In addition PSC exhibited lower values of average corrosion current density than those exhibited by OPC. Further the rate of increase in corrosion current density with free chloride content is less in PPC than PSC followed by OPC as indicated by the corresponding slopes of relationships shown in Fig. 9. Thus by looking at individual performances, Tempcore TMT steel performed best followed by Thermex TMT and CTD steels whereas in cement type, PPC performed best followed by PSC and OPC.

For the purpose of comparing the performance of different combination of steel and cement, the average corrosion current density values for given combinations at different free chloride contents were calculated by averaging over three w/c ratios and replicates. These calculated average corrosion current density values were plotted against the corresponding free chloride contents for all the nine combinations of steel and cement and are shown in Fig. 10. The relationships between corrosion current density and the free chloride contents from nine combinations are shown in Table 3. From Fig. 10, it is observed that, the combination of Tempcore TMT–PPC showed lower corrosion current density values as compared to other eight steel–cement combinations at all levels of free chloride contents. On the other hand, the combination of Thermex TMT–OPC exhibited higher values of corrosion current density as compared to other combinations.

The corrosion current density values obtained thorough LPR measurements at the age of 1 year for all the specimens were slightly lower than those obtained at the age of 60 days and the average reduction is less than 3% irrespective of cement type, steel type, chloride content and w/c ratio. However the variation in corrosion current density values obtained by LPR method for some of the specimens at the ages of 90 days and 120 days with those obtained at the age of 60 days is not systematic with a maximum variation being ±5% and hence insignificant. In addition, the differences in average values of corrosion current density at 60 days, 90 days and 120 days are within the scatter of each set of data. For all cases, the maximum values of standard deviations of corrosion current density at 60 days, 90 days, and 120 days for admixed chloride contents of 0%, 0.91%, 1.82% and 2.73% are 0.12 μA/cm², 0.15 μA/cm², 0.22 μA/cm² and 0.21 μA/cm², respectively. A typical histogram plot of corrosion current density versus admixed chloride content showing the variation at ages of 60 days, 90 days, and 120 days for Thermex TMT steel in PPC at w/c ratio of 0.5 is shown in Fig. 11. Thus the corrosion current density values remained almost constant through out the 1 year period of observa-

Table 3
Relationship between corrosion current density (y) and free chloride content (x) for steel–cement combinations.

Steel–cement combinations	Relationship	Regression coefficient (R)
Tempcore TMT–PPC	$y = 10.231x + 1.2665$	0.956
Thermex TMT–PPC	$y = 9.1682x + 2.509$	0.992
Tempcore TMT–PSC	$y = 9.8684x + 2.5814$	0.999
CTD–PPC	$y = 10.233x + 2.8535$	0.977
Thermex TMT–PSC	$y = 14.786x + 2.163$	0.929
Tempcore TMT–OPC	$y = 15.532x + 2.5695$	0.975
CTD–PSC	$y = 18.592x + 2.2702$	0.943
CTD–OPC	$y = 19.94x + 2.7036$	0.900
Thermex TMT–OPC	$y = 27.181x + 1.2617$	0.945

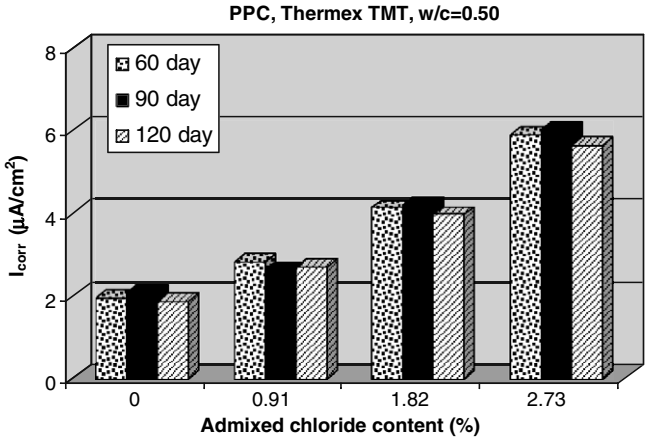

Fig. 11. Corrosion current density versus admixed chloride at 60 days, 90 days and 120 days

tion. The average values of I_{corr} obtained through LPR at 60 days and 1 year are considered as the average corrosion rate over this period for all the specimens.

3.2. Comparison of corrosion rate by LPR and AC impedance spectroscopy

Corrosion current density values obtained through AC impedance spectroscopy at the age of 60 days are compared with those obtained by LPR technique at the same age. Histogram plots showing the comparison of corrosion current density values obtained from two methods for Tempcore TMT steel, Thermex TMT steel and CTD steel in three types of cement are shown in Figs. 12–14, respectively. From the results it is observed that the values of corrosion current density obtained by AC impedance spectroscopy were lower than those obtained by LPR method in all cases as evident from Figs. 12–14. On an average corrosion current density values measured by AC impedance technique with the assumed steel–concrete interface model were about 9% lower than those measured by LPR method. However the variation in corrosion current density values with experimental parameters, i.e. steel type, cement type and chloride content was similar in both methods. A

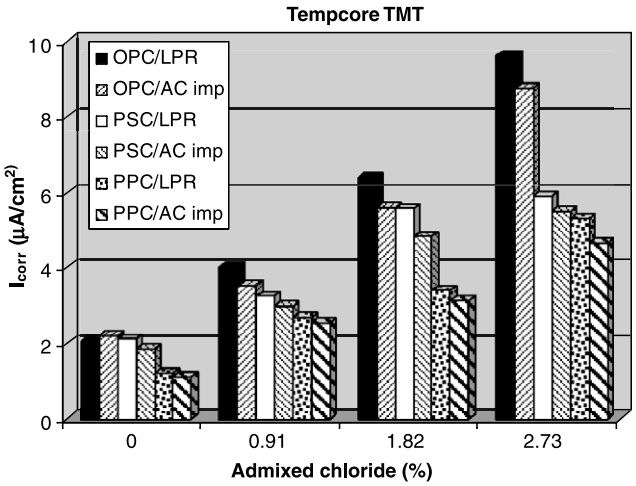

Fig. 12. Comparative plot of I_{corr} from LPR and AC impedance for Tempcore TMT steel.

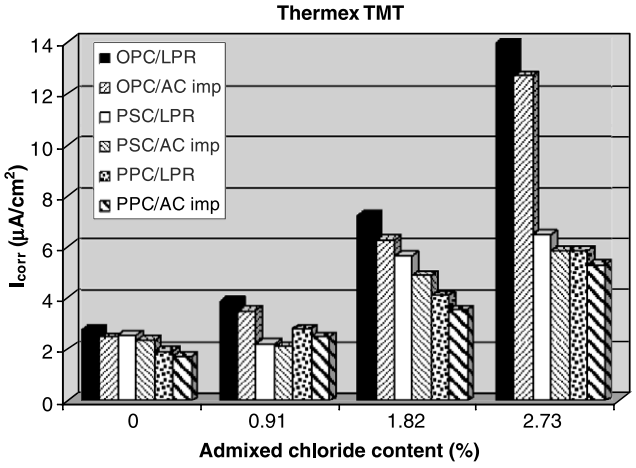

Fig. 13. Comparative plot of I_{corr} from LPR and AC impedance for Thermex TMT steel.

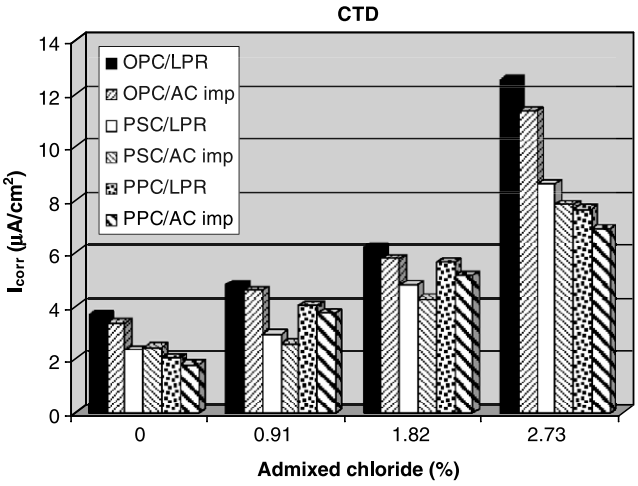

Fig. 14. Comparative plot of I_{corr} from LPR and AC impedance for CTD steel.

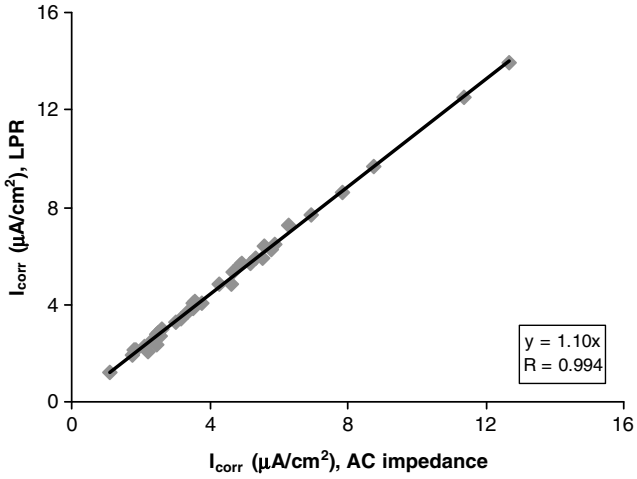

Fig. 15. Variation between LPR-I_{corr} and AC impedance-I_{corr}.

plot of corrosion current density values measured by LPR technique versus the corresponding corrosion current density values measured by AC impedance technique for all 36 (three types of steel, three types of cement and four chloride contents) cases is shown in Fig. 15. A strong linear correlation exists between the corrosion current density values measured by these two methods as indicated by the '*R*' (regression coefficient) value of 0.994. Thus the variation is almost completely represented by the linear relationship, i.e. $I_{corr}(LPR) = 1.10 \times I_{corr}(AC\ impedance)$ and further almost all points are on the best fit line as shown in Fig. 15.

3.3. Comparison of corrosion rate by LPR and gravimetric measurement

The steel specimens just after removal from slabs were visually observed and the photograph of some steel specimens is shown in Fig. 16. The extent of corrosion was more on steel specimens removed from the slabs made with OPC than PPC and PSC. Similarly Tempcore TMT steel showed less extent of corrosion than Thermex TMT and CTD steels as observed visually. The measured mass losses of the steel specimens as stated earlier were more in OPC than PPC and PSC. Similarly the measured mass losses of Tempcore TMT steel specimens were lower than those of Thermex TMT and CTD steel specimens. Therefore the blended cements, i.e. PPC and

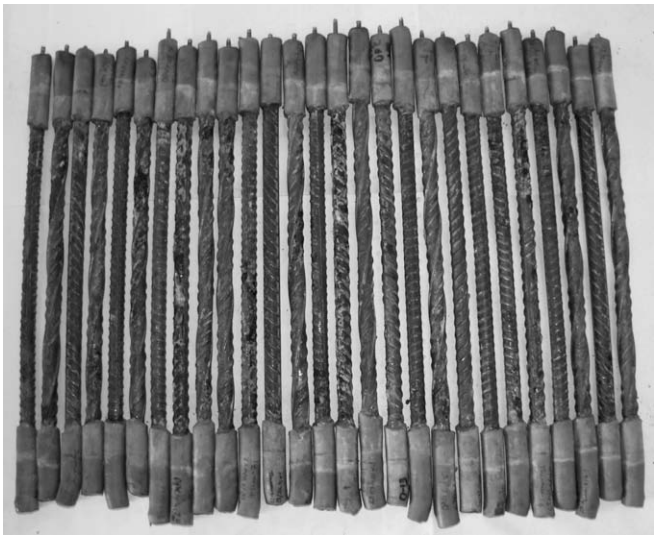

Fig. 16. Steel specimens just after removal from slabs.

PSC and Tempcore TMT steel performed better than OPC and Thermex TMT and CTD steels respectively against chloride induced corrosion.

From the results of average corrosion current density obtained by LPR technique and gravimetric method at the age of 1 year, it was observed that the percentage variation in values of corrosion current density obtained by these two methods for all experimental combinations lies mostly within ±10%. However the variation in corrosion rate values with cement type, steel type, w/c ratios and chloride contents was similar in both methods. Histogram plots showing the comparison of average corrosion current density values by LPR method and the corrosion current density values obtained by gravimetric method for Tempcore TMT steel in three types of cement at w/c ratios of 0.45, 0.50 and 0.55, are shown in Figs. 17–19, respectively. Similarly the corresponding plots for Thermex TMT steel and CTD steel in three types of cement at the above three w/c ratios are shown in Figs. 20–25, respectively. From these plots it is observed that there is close agreement of results obtained from the non-destructive linear polarization resistance with the actual mass loss results.

A plot of corrosion current density values obtained by LPR method against the corresponding corrosion current density values

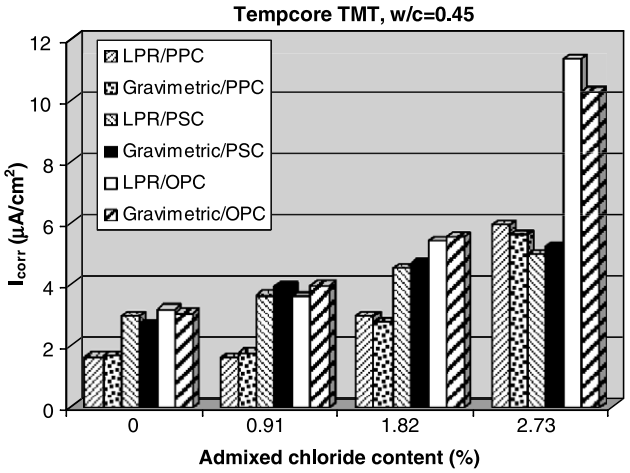

Fig. 17. Comparative plot of I_{corr} from LPR and gravimetric method for Tempcore TMT steel at w/c of 0.45.

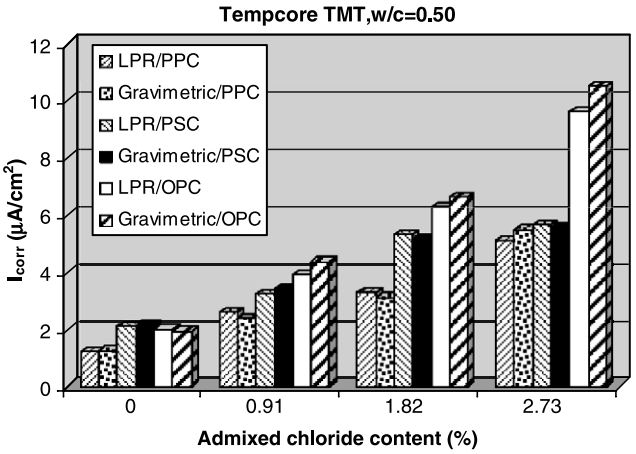

Fig. 18. Comparative plot of I_{corr} from LPR and gravimetric method for Tempcore TMT steel at w/c of 0.50.

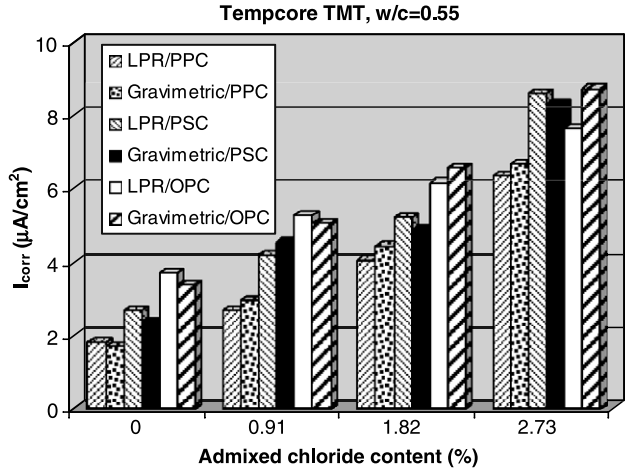

Fig. 19. Comparative plot of I_{corr} from LPR and gravimetric method for Tempcore TMT steel at w/c of 0.55.

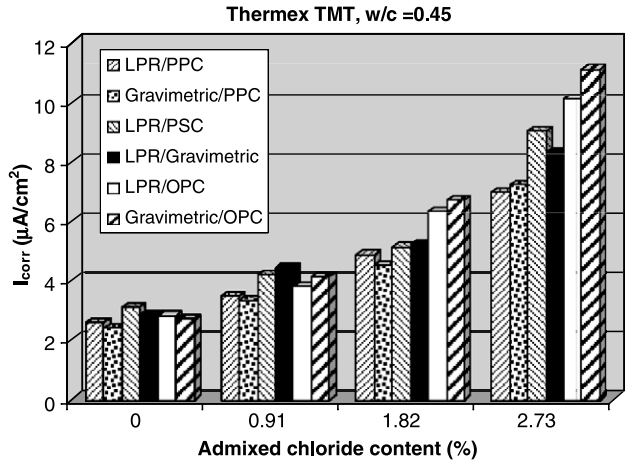

Fig. 20. Comparative plot of I_{corr} from LPR and gravimetric method for Thermex TMT steel at w/c of 0.45.

by gravimetric method for all 108 (three types of steel, three types of cement, three w/c ratios and four chloride contents) cases is shown in Fig. 26. From this figure it is observed that variation in the corrosion current density values from these two methods is

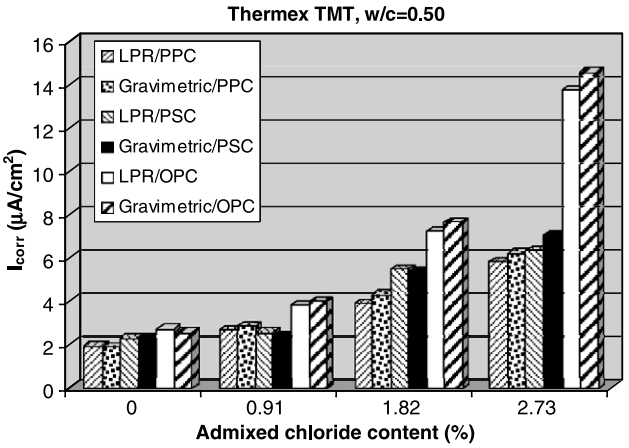

Fig. 21. Comparative plot of I_{corr} from LPR and gravimetric method for Thermex TMT steel at w/c of 0.50.

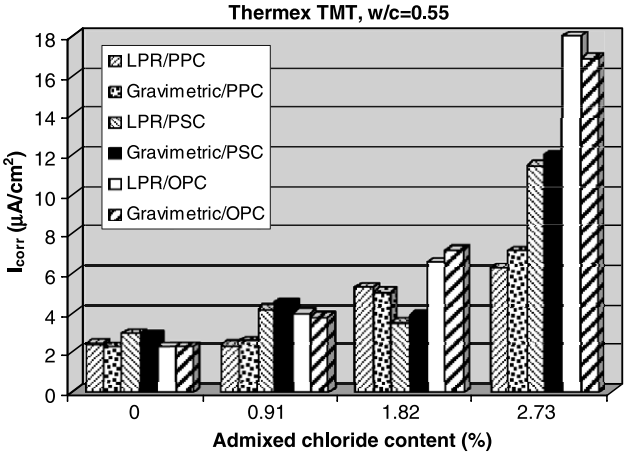

Fig. 22. Comparative plot of I_{corr} from LPR and gravimetric method for Thermex TMT steel at w/c of 0.55.

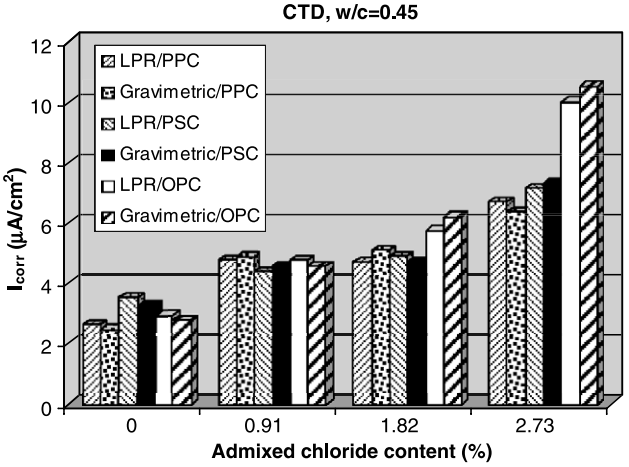

Fig. 23. Comparative plot of I_{corr} from LPR and gravimetric method for CTD steel at w/c of 0.45.

very less as evident from the relationship shown, i.e. $I_{corr}(LPR) = 0.99 \times I_{corr}(gravimetric)$ and corresponding '*R*' (regression coefficient) value is also very high, i.e. 0.989. The percentage variation in corrosion current density values between LPR and gravimetric method for Tempcore TMT steel, Thermex TMT steel, and CTD steel

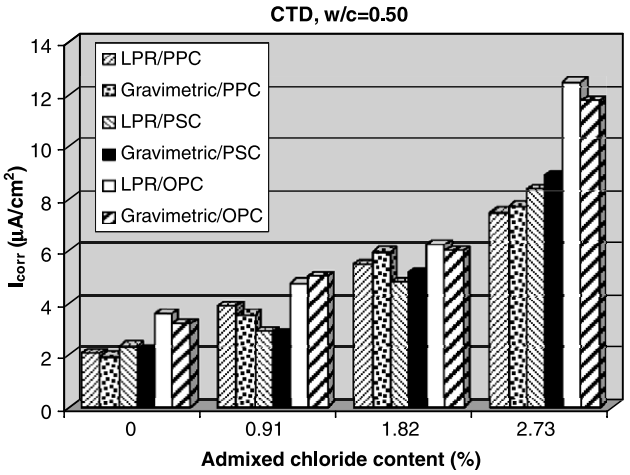

Fig. 24. Comparative plot of I_{corr} from LPR and gravimetric method for CTD steel at w/c of 0.50.

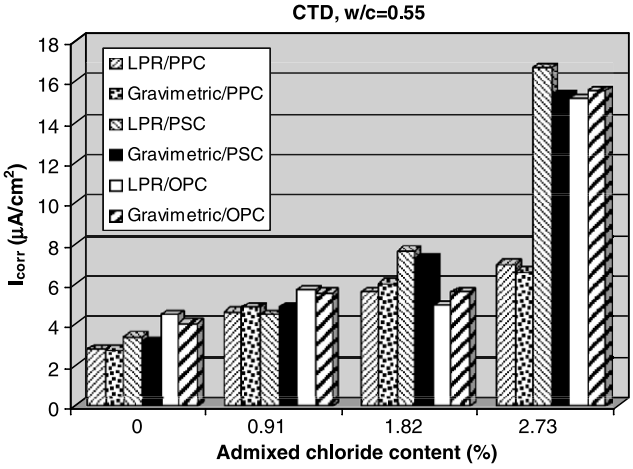

Fig. 25. Comparative plot of I_{corr} from LPR and gravimetric method for CTD steel at w/c of 0.55.

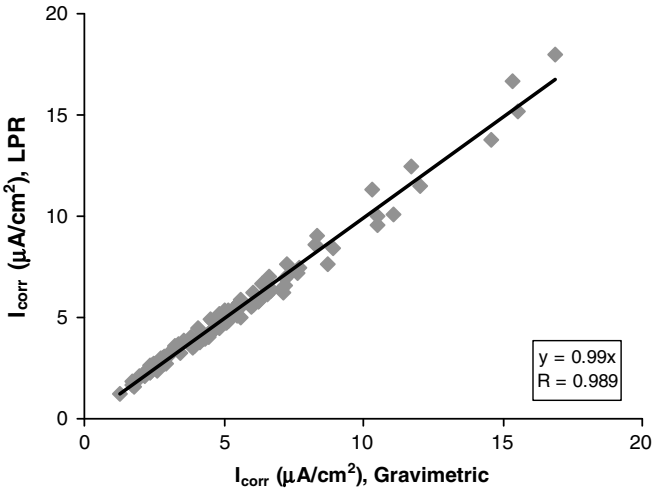

Fig. 26. Variation between LPR-I_{corr} and gravimetric-I_{corr}.

are shown in Figs. 27–29, respectively in three types of cement, three w/c ratios and four admixed chloride contents. From these plots it is observed that the average percentage variation between

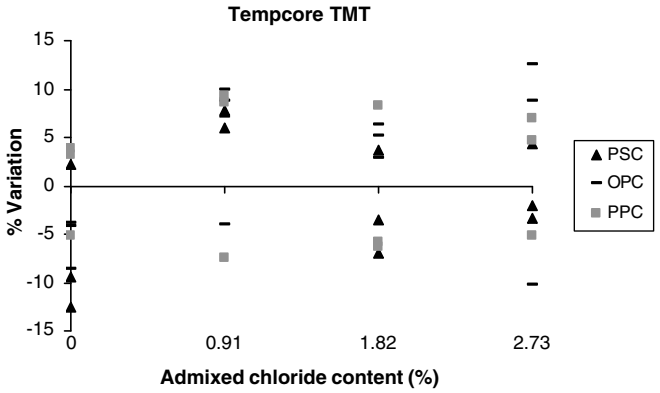

Fig. 27. Variation (%) in I_{corr} between LPR and gravimetric method for Tempcore TMT steel in PSC, OPC, and PPC.

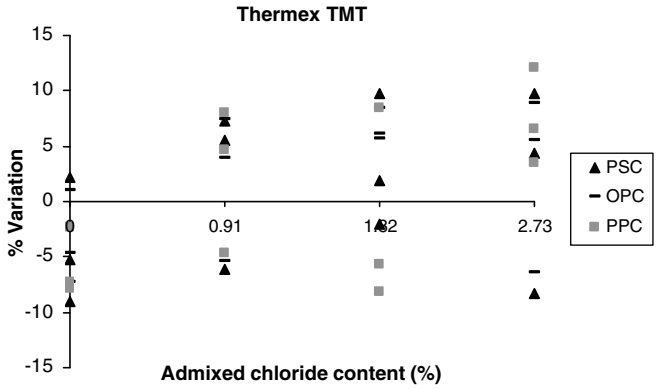

Fig. 28. Variation (%) in I_{corr} between LPR and gravimetric method for Thermex TMT steel in PSC, OPC, and PPC.

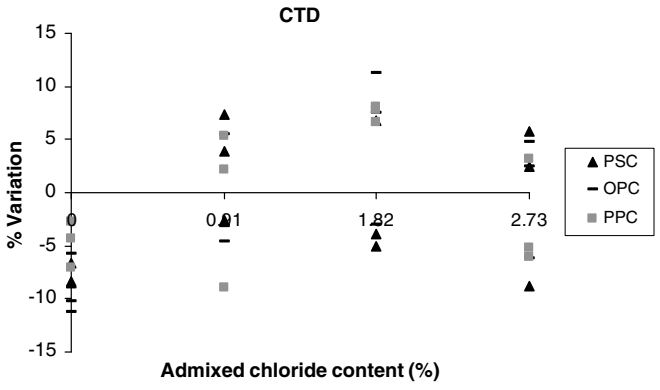

Fig. 29. Variation (%) in I_{corr} between LPR and gravimetric method for CTD steel in PSC, OPC, and PPC.

two methods is about ±6%, the maximum being 12% and further the percentage variation is independent of steel type, cement type and mix parameters as evident from these plots.

3.4. Analysis of variance (ANOVA)

The analysis of variance allows in evaluating whether an independent variable has an effect on the dependent variable or not. In addition, it can also be used to identify whether the interactions of independent variables have an effect on the dependent variable or not. Sometimes it may be difficult to analyze the effect of different factors on the variation of dependent variables; ANOVA results can be useful to see the effect. The ANOVA calculations in the present work have been carried out according to the guidelines presented by Hicks [26]. The corrosion rate values of three replicates for each specimen obtained through LPR technique at four levels of admixed chloride contents for three types of cement, three types steel, three w/c ratios, and two testing ages (60 days and 1 year) are arranged in a tabular form. After that the total sum of squares is calculated, which is partitioned into the sum of squares (SS) for individual factors and the sum of the squares for the residual random error. Then the mean squares (MS) of the factors are calculated by dividing their corresponding sum of squares by the associated degrees of freedom (df). Then the effect of individual factors is evaluated by testing the hypothesis of equality of variances, which is the test of null hypothesis or simply the significance test at a particular probability level. For this, the ratio of mean squares of factors to the mean squares of the residual error, i.e. *F*-statistic is calculated and compared to the tabulated *F*-values related to Fisher distribution. The *F*-values related to Fisher distribution depend upon the number of degrees of freedom of the individual factors, number of degrees of freedom of the residual error and the probability level and are available in tabular form in relevant texts [26]. The results of ANOVA for corrosion current density are presented in Table 4. From this table it is observed that for all other factors except age, the calculated *F*-values are higher than the corresponding tabulated *F*-values at 99% confidence level. This indicates that except age, all other factors, i.e. chloride content, steel type, cement type, and w/c ratio are affecting the corrosion rate and this further confirms that corrosion rate remained almost constant with age of testing adopted in the investigation. Among all factors, chloride content has the strongest effect on corrosion rate than other factors followed by cement type, steel type and w/c ratio as evident from Table 4.

Table 4
ANOVA results for corrosion current density.

Source	Level	Degree of freedom (df)	Sum of squares (SS)	Mean squares (MS)	*F*-ratio	'*F*' from Fisher's distribution at 99% probability
Cement type	3	2	586.82	293.41	124.38	4.61
Testing age	2	1	2.10	2.10	0.89	6.63
Steel type	3	2	206.56	103.28	43.78	4.61
Chloride content	4	3	3769.35	1256.45	532.61	3.78
w/c ratio	3	2	141.12	70.56	29.91	4.61
Error		637	1502.70	2.36		
Totals		647	6208.65			

3.5. Performance of cement and steel type

The lower corrosion rate in blended cements, i.e. PPC and PSC as compared to that in OPC is due to the increase in the resistivity value of concrete. This increase in resistivity in blended cements is due to the formation of additional C–S–H gels that results in the formation of finer pore structure and thereby resulting in a denser microstructure in the hardened concrete. Further the reduction of concentrations of Ca^{++} and OH^{-} ions in blended cements due to consumption by pozzolana, may have reduced the electrolytic conductivity of the concrete pore solution and hence resulting in higher resistivity and less corrosion rate.

The Tempcore TMT steel exhibited lower corrosion rates as compared to Thermex TMT and CTD steels. It is known that, the CTD bar exhibits higher residual internal stress [27], that is introduced by cold work and these results in a higher tendency for CTD steels to go into anodic dissolution than that for TMT steels,

owing to their less residual internal stress. Further the kinetics of dissolution of iron ions in to solution would also depend upon the surface microstructure of the steel bar. Martensite being a hard phase compared to stressed ferrite–pearlite, its rate of dissolution is also likely to be lower. Thus TMT steels are likely to exhibit lower corrosion rate than CTD steel. The degree of tempering, thickness and surface microstructure of the tempered martensite layer may be different for Tempcore and Thermex TMT steels. This may have resulted in improved corrosion resistance of Tempcore TMT steel than Thermex TMT steel.

The better performance of the combination of Tempcore TMT steel and PPC in terms of exhibiting lower corrosion density is due to their combined effects of improved performances as already mentioned. The poor performance of combination of Thermex TMT and OPC may be due to the poor performance of OPC being more dominant than Thermex TMT steel.

4. Conclusions

From the results of the present investigation, following conclusions were drawn:

(1) The corrosion current density values obtained by AC impedance spectroscopy technique are slightly lower than those obtained by linear polarization technique. The average percentage reduction in the values of corrosion current density is about 9%. However the variations in the values of corrosion current density with steel type, cement type and mix parameters are similar in both methods.

(2) The values of corrosion current density obtained by linear polarization resistance technique with guard ring electrode are in close agreement with those obtained from gravimetric (mass loss) measurement. The average percentage variation in values by two techniques is about ±6%. In addition, the variations in the values of corrosion current density with cement type, steel type and mix parameters are similar in both techniques. Therefore it is concluded that LPR technique serves as a suitable non-destructive method for determination of corrosion rate. Thus the inferences drawn based on LPR results are further confirmed.

(3) From the results of corrosion rate obtained by three different techniques, it was concluded that the blended cements, i.e. PPC and PSC performed better as compared to OPC against chloride induced rebar corrosion in concrete whereas, amongst steel type Tempcore TMT steel resulted in lower corrosion rate as compared to Thermex steel followed by CTD steel.

(4) From the results of ANOVA, it was concluded that chloride content has the strongest effect on corrosion rate followed by cement type, steel type and w/c ratio. Further the corrosion rate remained almost constant with age of testing adopted in the investigation which is further confirmed through the results of ANOVA.

References

[1] Melchers RE, Li CQ. Phenomenological modeling of reinforcement corrosion in marine environments. ACI Mater J 2006;103:25–32.
[2] Almusallam AA. Effect of degree of corrosion on the properties of reinforcing steel bars. Constr Build Mater 2001;15:361–8.
[3] Maheswaran T, Sanjayan JG. A semi-closed-form solution for chloride diffusion in concrete with time-varying parameters. Mag Concr Res 2004;56:359–66.
[4] Elsener B. Macrocell corrosion of steel in concrete-implications for corrosion monitoring. Cem Concr Compos 2002;24:65–72.
[5] El-Gelany MA. Short-term corrosion rate measurement of OPC and HPC reinforced concrete specimens by electrochemical techniques. Mater Struct 2001;34:426–32.
[6] Liu T, Weyers RW. Modeling the dynamic corrosion process in chloride contaminated concrete structures. Cem Concr Res 1998;28:365–79.
[7] Hope BB, Page JA, Ip AKA. Corrosion rates of steel in concrete. Cem Concr Res 1986;16:771–81.
[8] Andrade C, Alonso C. Corrosion rate monitoring in the laboratory and on-site. Constr Build Mater 1996;10:315–28.
[9] Law DW, Millard SG, Bungey JH. Effect of electrode orientation on linear polarisation measurements using sensor controlled guard ring. Br Corros J 2000;35(2):136–40.
[10] Law DW, Millard SG, Bungey JH. Linear polarisation resistance measurements using a potentiostatically controlled guard ring. NDT&E Int 2000;33(1):15–21.
[11] Gu GP, Beaudoin JJ, Ramachandran VS. Techniques for corrosion investigation in reinforced concrete. In: Ramachandran VS, Beaudoin JJ, editors. Handbook of analytical techniques in concrete science and technology. New Jersey: Noyes Publications; 2001. p. 441–504.
[12] Ismail M, Ohtsu M. Corrosion rate of ordinary and high-performance concrete subjected to chloride attack by AC impedance spectroscopy. Constr Build Mater 2006;20:458–69.
[13] Jones DA. Principles and prevention of corrosion. Upper Saddle River (NJ): Prentice Hall; 1996.
[14] Montemor MF, Simoes AMP, Ferreira MGS. Chloride-induced corrosion on reinforcing steel: from the fundamentals to the monitoring techniques. Cem Concr Compos 2003;25:491–502.
[15] IS 383-1970 (Reaffirmed 2002). Specification for coarse and fine aggregates from natural sources for concrete. New Delhi: Bureau of Indian Standards.
[16] Neville AM, Brooks JJ. Concrete technology. Delhi: Pearson Education; 2004.
[17] ASTM G 109-99a (Reapproved 2005). Standard test method for determining the effects of chemical admixtures on the corrosion of embedded steel reinforcement in concrete exposed to chloride environments. West Conshohocken, PA.
[18] Pradhan B, Bhattacharjee B. Role of steel and cement type on chloride-induced corrosion in concrete. ACI Mater J 2007;104:612–9.
[19] Dehwah HAF, Maslehuddin M, Austin SA. Long-term effect of sulfate ions and associated cation type on chloride-induced reinforcement corrosion in Portland cement concretes. Cem Concr Compos 2002;24:17–25.
[20] Saricimen H, Mohammad M, Quddus A, Shameem M, Barry MS. Effectiveness of concrete inhibitors in retarding rebar corrosion. Cem Concr Compos 2002;24:89–100.
[21] Erdogdu S, Bremner TW, Kondratova IL. Accelerated testing of plain and epoxy-coated reinforcement in simulated seawater and chloride solutions. Cem Concr Res 2001;31:861–7.
[22] Andion LG, Garces P, Cases F, Andreu CG, Vazquez JL. Metallic corrosion of steels embedded in calcium aluminate cement mortars. Cem Concr Res 2001;31:1263–9.
[23] Dhir RK, Jones MR, McCarthy MJ. PFA concrete: chloride-induced reinforcement corrosion. Mag Concr Res 1994;46:269–77.
[24] ASTM G 1-03. Standard practice for preparing, cleaning, and evaluating corrosion test specimens. West Conshohocken, PA; 2003.
[25] Trejo D, Monteiro PJ. Corrosion performance of conventional (ASTM A615) and low-alloy (ASTM A706) reinforcing bars embedded in concrete and exposed to chloride environments. Cem Concr Res 2005;35:562–71.
[26] Hicks CR. Fundamental concepts in the design of experiments. 3rd ed. New York: Holt, Rinehart and Winston; 1982.
[27] Saha JK. Guidebook on proper usage of steel reinforcement bars for durable construction practices. Kolkata, India: Institute for Steel Development and Growth; 2005, INS/PUB/075.